Targeted Disruption of the Murine Na^+/H^+ Exchanger Isoform 2 Gene Causes Reduced Viability of Gastric Parietal Cells and Loss of Net Acid Secretion

Patrick J. Schultheis,* Lane L. Clarke,‖ Pierre Meneton,* Matthew Harline,‖ Gregory P. Boivin,§ Grant Stemmermann,§ John J. Duffy,* Thomas Doetschman,* Marian L. Miller,‡ and Gary E. Shull*

**Department of Molecular Genetics, Biochemistry and Microbiology, ‡Department of Environmental Health, and §Department of Pathology and Laboratory Medicine, University of Cincinnati College of Medicine, Cincinnati, Ohio 45267-0524; and ‖Department of Veterinary Biomedical Sciences, Dalton Cardiovascular Research Center, University of Missouri, Columbia, Missouri 65211*

Abstract

Multiple isoforms of the Na^+/H^+ exchanger (NHE) are expressed at high levels in gastric epithelium, but the physiological role of individual isoforms is unclear. To study the function of NHE2, which is expressed in mucous, zymogenic, and parietal cells, we prepared mice with a null mutation in the NHE2 gene. Homozygous null mutants exhibit no overt disease phenotype, but the cellular composition of the oxyntic mucosa of the gastric corpus is altered, with parietal and zymogenic cells reduced markedly in number. Net acid secretion in null mutants is reduced slightly relative to wild-type levels just before weaning and is abolished in adult animals. Although mature parietal cells are observed, and appear morphologically to be engaged in active acid secretion, many of the parietal cells are in various stages of degeneration. These results indicate that NHE2 is not required for acid secretion by the parietal cell, but is essential for its long-term viability. This suggests that the unique sensitivity of NHE2 to inhibition by extracellular H^+, which would allow upregulation of its activity by the increased interstitial alkalinity that accompanies acid secretion, might enable this isoform to play a specialized role in maintaining the long-term viability of the parietal cell. (*J. Clin. Invest.* 1998. 101:1243–1253.) Key words: embryonic stem cells • gene targeting • mucosal protection • ion transport • stomach

Introduction

Secretion of hydrochloric acid in the stomach poses formidable problems for the gastric epithelium with regard to both the mechanisms of acid secretion and the mechanisms for maintaining epithelial cell viability. Available evidence suggests that basolateral Na^+/H^+ exchangers (NHEs)[1] play a role in each of these processes (1–7). Northern blot analyses of mRNA from purified preparations of the three major gastric epithelial cell types from both rat and rabbit have shown that NHE isoforms 1, 2, and 4 are expressed in parietal, chief, and mucous cells (8). Thus, the basolateral Na^+/H^+ exchange activity identified in each of these cell types (1, 2, 4–6) could represent the activities of any one or a combination of these isoforms. However, the precise role of NHEs in acid secretion and mucosal protection is poorly understood, and little is known about the function of individual isoforms.

With regard to acid secretion, it has been suggested that NHEs on the basolateral membrane of the parietal cell mediate the influx of Na^+ that is required as a counterion for K^+ uptake via the Na^+,K^+-ATPase (1, 2), and that coupled Na^+/H^+ and Cl^-/HCO_3^- exchange is involved in the maintenance of high intracellular Cl^- concentrations required for HCl and KCl secretion across the apical membrane (2, 3). Basolateral NHEs play an important role in mucosal protection by extruding protons that diffuse into mucous and chief cells from the acidic luminal fluid (4–6), and may also contribute to the intracellular conditions needed for apical secretion of HCO_3^- by mucous cells, which maintains the alkalinity of the mucous coating (9, 10). A potential role of the NHEs in maintaining parietal cell viability is to contribute, via coupling with other transporters, to the maintenance of membrane potential, and intracellular pH, electrolyte, and volume homeostasis of the parietal cell during acid secretion. This may be particularly important given the potential for acid secretion to overwhelm the mechanisms for maintaining homeostasis of the gastric parietal cell.

Na^+/H^+ exchanger isoform 2 (NHE2) is present in all three of the major gastric epithelial cell types (8), and is also expressed in small intestine, colon, kidney, and several other tissues (11, 12). NHE2 has been well-characterized with respect to its biochemical properties (13), but its physiological functions remain unclear. A comprehensive understanding of the role of NHE2 in gastric epithelium, as well as in other tissues, will require an explanation of the relationship between its unique biochemical characteristics and its physiological function. NHE2 exhibits a 10-fold greater sensitivity to inhibition by extracellular protons than NHE1 and NHE3 (13, 14). This unusual biochemical property suggests that NHE2 might be activated in response to the increased alkalinity that occurs on the basal side of the gastric epithelium during stimulation of acid secretion. In fact, there is evidence for upregulation of Na^+/H^+ exchange on the basolateral membrane of the parietal cell in response to increased interstitial pH and HCO_3^- (7). In

Address correspondence to Gary E. Shull, Department of Molecular Genetics, Biochemistry and Microbiology, University of Cincinnati College of Medicine, Bethesda Avenue, ML 524, Cincinnati, OH 45267-0524. Phone: 513-558-0056; FAX: 513-558-1885; E-mail: gary.shull@uc.edu P. Meneton's current address is INSERM U367, 17 Rue du Fer a Moulin, 75005 Paris, France.

Received for publication 21 July 1997 and accepted in revised form 16 January 1998.

J. Clin. Invest.

0021-9738/98/03/1243/11 $2.00
Volume 101, Number 6, March 1998, 1243–1253
http://www.jci.org

1. *Abbreviations used in this paper:* ES, embryonic stem; NHE, Na^+/H^+ exchanger (specific isoforms are designated NHE1, NHE2, NHE3, or NHE4); $NHE2^{-/-}$, $NHE2^{+/-}$, and $NHE2^{+/+}$, NHE2 homozygous mutant, heterozygous mutant, and wild-type, respectively; RT, reverse transcriptase; TUNEL, terminal deoxynucleotidyltransferase–mediated, dUTP nick end labeling.

addition, there is evidence that HCO_3^- extruded across the basolateral membrane of the actively secreting parietal cell plays a major role in mucosal protection by enhancing the capabilities of mucous cells for apical HCO_3^- secretion (10) and H^+ disposal (15), both of which are likely to involve basolateral Na^+/H^+ exchange. Thus, increased activity of NHE2 in response to extracellular alkalinity could allow this isoform to play important roles in acid secretion, parietal cell viability, and mucosal protection. To examine the physiological functions of NHE2 in stomach, we developed and analyzed a mouse model with a null mutation in the NHE2 gene.

Methods

Preparation of targeting construct. A genomic clone containing part of the mouse NHE2 gene was isolated from a library constructed with DNA from mouse strain 129/SvJ and the λ DASH phage vector. An 8.0-kb HindIII fragment containing exon 2, which encodes amino acids 99–252, was used to prepare the targeting construct; digestion with PvuII, for which there is a single restriction site at codon 217 in exon 2, yielded two fragments, 3.3 and 4.7 kb in size. These fragments were blunt-end ligated into BamHI and XhoI sites that flank the neomycin resistance gene in the targeting vector MJK^+KO (a kind gift of Dr. Steven Potter, Children's Hospital Medical Center, Cincinnati, OH), which also contains the herpes simplex virus thymidine kinase gene.

Embryonic stem (ES) cell culture, electroporation, and selection of targeted cells. ES cells were cultured on a feeder layer of embryonic fibroblasts in DME supplemented with 15% FBS, 2 mM glutamine, and 0.1 mM β-mercaptoethanol. ES cells were dispersed by trypsin digestion, washed, and resuspended in PBS at 2×10^7 cells/ml, and then 0.6 ml was electroporated with 5 nM targeting construct DNA (linearized at a NotI site located in the vector sequence immediately 5′ to the NHE2 genomic sequence). After 2 min, the electroporated cells were brought to 10 ml with culture media and seeded onto fibroblast feeder layers at 1.2×10^6 cells per 100-mm dish. 1 d after electroporation, G418 was added to a final concentration of 500 μg/ml, and after 24 h, was reduced to 250 μg/ml for the remainder of the selection period. Starting on day 2, the cells were also exposed to 2 μM gancyclovir for 4 d. This positive–negative selection strategy allowed the growth of cells containing the neomycin resistance gene but lacking the herpes simplex virus thymidine kinase gene, thereby enriching for colonies derived from a homologous recombination event. ES cell colonies resistant to both drugs were isolated on day 11; clonal isolates were split 6 d later onto two sets of 24-well plates. The samples in one set of wells were used for preparation of genomic DNA, and those in the other set were placed in frozen storage.

Southern blot analysis and generation of mutant animals. ES cell DNA was isolated from individual clonal isolates that were resistant to both G418 and gancyclovir, and analyzed by Southern blot analysis using probes derived from genomic DNA located immediately 5′ and 3′ of the HindIII fragment used to prepare the construct. The 5′ probe was a 0.3-kb PvuII-HindIII fragment, which hybridized with 3.6- and 4.5-kb PvuII fragments in the wild-type and mutant genes, respectively. The 3′ probe was a 0.8-kb HindIII-SstI fragment, which hybridized with 6.7-and 5.6-kb SstI fragments in the wild-type and mutant genes, respectively. Four targeted ES cell lines were injected into C57Bl6 blastocysts, and the chimeric blastocysts were implanted into pseudopregnant ICR female mice. Male chimeras resulting from this procedure were bred with female Black Swiss mice. Heterozygous offspring, identified by Southern blot and/or PCR analysis of DNA isolated from tail biopsies of animals with the ES cell–derived agouti coat color, were bred to establish a colony carrying the mutant NHE2 gene.

Northern blot analysis. Total RNA was isolated from tissues of 10-wk-old mice using Tri Reagent® as described by the supplier (Molecular Research Center, Inc., Cincinnati, OH). RNA (10 μg) was denatured with glyoxal and dimethyl sulfoxide, fractionated by electrophoresis in 1% agarose, and transferred to a nylon membrane. Hybridization with ^{32}P-labeled cDNA probes and washes were performed by the method of Church and Gilbert (16). The cDNA probes used for the Northern blot analyses were (*a*) rat NHE2, a 3.1-kb fragment spanning nucleotides 449–3561; (*b*) rat gastric H^+,K^+-ATPase α-subunit, a 0.7-kb fragment spanning nucleotides 2676–3305; (*c*) rat pepsinogen, a 1.2-kb fragment spanning nucleotides 67–1224; and (*d*) mouse gastrin, a 368-bp fragment spanning nucleotides 16–383.

Reverse transcriptase (RT) PCR and sequence analysis of wild-type and mutant NHE2 mRNAs. RNA from wild-type and mutant tissues was reverse transcribed with Superscript II RNase H^- reverse transcriptase (GIBCO BRL, Gaithersburg, MD) using a primer complementary to codons 328–336 in exon 3. Amplification of the first strand cDNA was performed using a primer corresponding to codons 80–88 in exon 1 and a reverse primer complementary to codons 264–272 in exon 3. PCR fragments were separated on a 2% agarose gel and visualized by staining with ethidium bromide. PCR products were analyzed by automated DNA sequencing.

Analysis of systemic acid-base and electrolyte status. Plasma pH and electrolytes were determined using a pH/blood gas analyzer (model 348; Chiron Diagnostics, Oberlin, OH). Mice were warmed gently under a heat lamp for 30 s to increase peripheral blood circulation. The tail vein was then nicked with a scalpel, and 50 μl of blood was collected in a heparinized capillary tube and analyzed immediately. Separate studies have shown that pH and electrolyte values obtained from the tail vein by this method are comparable to those for blood collected by intraarterial catheterization. Aldosterone levels were determined using an ^{125}I RIA kit (Diagnostic Products Corp., Los Angeles, CA).

Microscopy and morphometry. Stomach, small intestine, large intestine, and kidney were fixed in 10% neutral buffered formalin, dehydrated through a gradient of alcohols, and embedded in paraffin. 5-μm-thick sections of each tissue were stained with hematoxylin and eosin and examined by light microscopy. For detailed light and transmission electron microscopy of gastric epithelium, stomachs were opened, washed gently, fixed in 4% paraformaldehyde in phosphate buffer (pH 7.3), postfixed in 1% osmium tetroxide in the same buffer, dehydrated in ethanol and propylene oxide, and embedded in Spurr's resin. Transverse 1 mm-thick slices were flat-embedded in Beem® capsules (Electron Microscopy Sciences, Fort Washington, PA), 1.5-μm-thick sections were stained with toluidine blue for light microscopy, and thin sections were stained with uranyl acetate and lead citrate for electron microscopy.

Light microscopic morphometry of stomach was performed at a magnification of 1,250 at a site along the greater curvature of the stomach between 4 and 5 mm from the pylorus. The glandular area of the stomach at the greater curvature was embedded so that sections could be cut perpendicular to the plane of the basement membrane, providing cross sections of the epithelium. Two or three gastric glands were included in each field, and 400–600 cells were counted per slide. Beginning at the base of a gland, the cells in the entire gland were counted. Cells with distinct zymogen granules, parietal cells, and other cells without distinguishing characteristics (mucous and undifferentiated cells) were tallied. In addition, necrotic parietal cells, mitotic cells, small rounded cells with coarse and/or finely granular cytoplasm (enteroendocrine cells), and eosinophilic cells, both within the epithelium and in the adjacent lamina propria, were counted. Thickness of the gastric epithelium was measured from 5–10 camera lucida profiles drawn from the basement membrane to the border of the lumen of the epithelium at a magnification of 16, and digitized using SigmaScan Pro software and digitizing tablet (Jandel Scientific Software, San Rafael, CA). Cell counts and measurements of epithelial thickness were performed without prior knowledge of the genotype or age of the animals, which ranged from 3 to 8 wk for paraffin-embedded sections ($n = 13$ for each genotype) and 3 to 16 wk for plastic-embedded sections ($n = 7$ for each genotype). Because there appeared to be no substantial age-related differences in the values

measured, the data were pooled for presentation in Table I. The data were analyzed using the general linear model (SAS Institute, Inc., Cary, NC).

Terminal deoxynucleotidyltransferase-mediated, dUTP nick end labeling (TUNEL) assay. Stomachs from four wild-type and four homozygous adult mutant mice (8–10 wk old) were fixed in buffered formalin and embedded in paraffin. Sections (4 μm) were deparaffinized with xylene, rehydrated through a graded series of ethanol, and permeabilized with proteinase K (20 μg/ml) for 15 min at 37°C. DNA was nick end labeled with dUTP-fluorescein using an In Situ Cell Death Detection kit (Boehringer Mannheim Biochemicals, Indianapolis, IN), and incorporated nucleotides were detected with an anti-fluorescein antibody conjugated with alkaline phosphatase using Fast Red as a substrate. Sections were counterstained with aqueous hematoxylin.

Measurement of gastric pH and output of acid-base equivalents. Measurement of gastric acid output was performed by a modification (17) of the method described by Wood and Dubois (18). Unless indicated otherwise, the age range of all mice was 84–133 d. The mice were fasted, with free access to water, for at least 2 h before experimentation. Each mouse was injected subcutaneously with a sterile solution of histamine HCl (2 μg/g body wt; Sigma Chemical Co., St. Louis, MO) in PBS. After 15 min, the mouse was killed and immediately dissected. The intact stomach was removed via a midline laparotomy after clamping the gastroesophageal and pyloric junctions. The stomach was then immersed in 2 ml of oxygen-saturated normal saline solution (22°C) and opened along the lesser curvature. After everting and rinsing, the stomach was removed, blotted dry with absorbent paper, and weighed. The tube containing the gastric contents was centrifuged at 500 *g* for 5 min, and the supernatant was decanted into a small cup for titration. After measuring the pH , the supernatant was titrated to pH 6.5 with 0.01 N NaOH or 0.01 N HCl. The pellet was weighed before and after overnight drying to estimate liquid remaining in the pelleted fraction. Results are expressed as microequivalents of H^+ or OH^- (HCO_3^-) per gram of stomach wet weight.

Gastrin RIA. Wild-type ($n = 7$) and homozygous mutant ($n = 9$) mice, ~ 6 mo old, were fasted overnight, anesthetized by intraperitoneal injection of 2.5% avertin in physiological saline (0.015 ml avertin/g body wt), and bled by cardiocentesis. Serum was prepared, and relative gastrin concentrations were analyzed using an ^{125}I RIA kit designed for quantitative analysis of human serum gastrin (Diagnostic Products Corp.). The gastrin assay yielded relative values, as the polyclonal antibody used in the assays was raised against human gastrin, and the assay was standardized using ^{125}I-labeled human gastrin in competition with an unlabeled human gastrin standard.

Results

Targeted disruption of the NHE2 gene. A replacement-type vector was used to disrupt exon 2 of the NHE2 gene in ES cells (Fig. 1 *A*). This exon seemed appropriate for targeted disruption, as it encodes amino acids 99–252, which span transmembrane domains two through seven of the protein. 200 ES cell clones survived positive–negative selection on G418 and gancyclovir, and 16 were shown to be targeted correctly by diagnostic Southern blot analysis similar to that shown in Fig. 1 *B*. Blastocyst-mediated transgenesis was performed, and six chimeric male mice were obtained and bred with wild-type females. Offspring to which ES cell–derived DNA was transmitted were identified by their agouti coat color, and pups carrying the mutant gene were identified by Southern blot analysis of DNA from tail biopsies. Heterozygous NHE2 mutant animals ($NHE2^{+/-}$) were mated, offspring were genotyped by Southern blot analysis as shown in Fig. 1 *B*, and live homozygous null mutants ($NHE2^{-/-}$) were obtained.

Northern blot analysis was performed on total RNA isolated from animals of all genotypes to ensure that the NHE2 gene was inactivated. RNA transcripts of the expected size were detected in stomach, small intestine, colon, and kidney of wild-type ($NHE2^{+/+}$) and heterozygous mutant mice, whereas a slightly truncated transcript was observed in $NHE2^{-/-}$ animals (Fig. 2 *A*). The truncated NHE2 mRNA was present at reduced levels in kidney, small intestine, and large intestine of $NHE2^{-/-}$ mice, relative to the levels of NHE2 mRNA observed in wild-type mice, but the mutant mRNA was expressed at high levels in $NHE2^{-/-}$ stomachs. RT-PCR and sequence analysis of the $NHE2^{+/+}$ and $NHE2^{-/-}$ transcripts showed that a cryptic donor splice site located within codon 172 in exon 2 was spliced to the acceptor site of exon 3 (Fig. 2 *B*). The aberrant splice deletes 241 nucleotides encoding amino acids 172–252, and causes a frameshift in the coding sequence (Fig. 2 *C*) that eliminates 641 amino acids of the 813–amino acid protein. The region that is eliminated includes nine of the twelve putative transmembrane domains and the extensive carboxy-terminal hydrophilic domain.

Gross phenotype. Genotype frequencies close to the normal 1:2:1 Mendelian ratios for wild-type, heterozygous, and homozygous mutants (114 +/+; 163 +/−; 78 −/−) were ob-

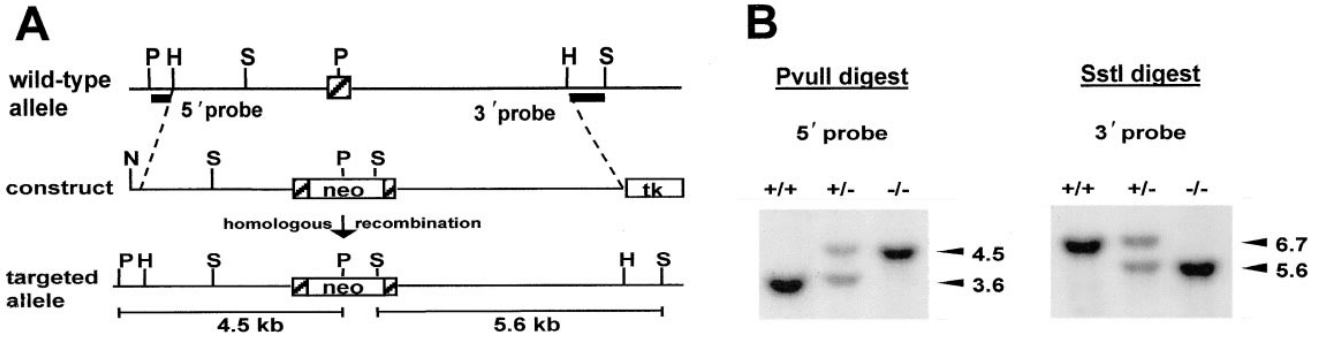

Figure 1. NHE2 gene targeting strategy and Southern blot analysis. (*A*) *Top*, map of the region of the wild-type gene that contains exon 2; *middle*, diagram of targeting construct, which was prepared using an 8-kb HindIII fragment; *bottom*, predicted structure of the targeted allele. 4.5-kb PvuII and 5.6-kb SstI restriction fragments that are unique to the targeted allele are indicated. *P*, PvuII. *S*, SstI. *H*, HindIII. *N*, NotI. *neo*, Neomycin resistance gene. *tk*, herpes simplex virus thymidine kinase gene. (*B*) Southern blot analysis of tail DNA isolated from representative offspring of a heterozygous mating. DNA was digested with either PvuII or SstI and hybridized with the 5′ and 3′ probes (*solid bars* in *A*), respectively.

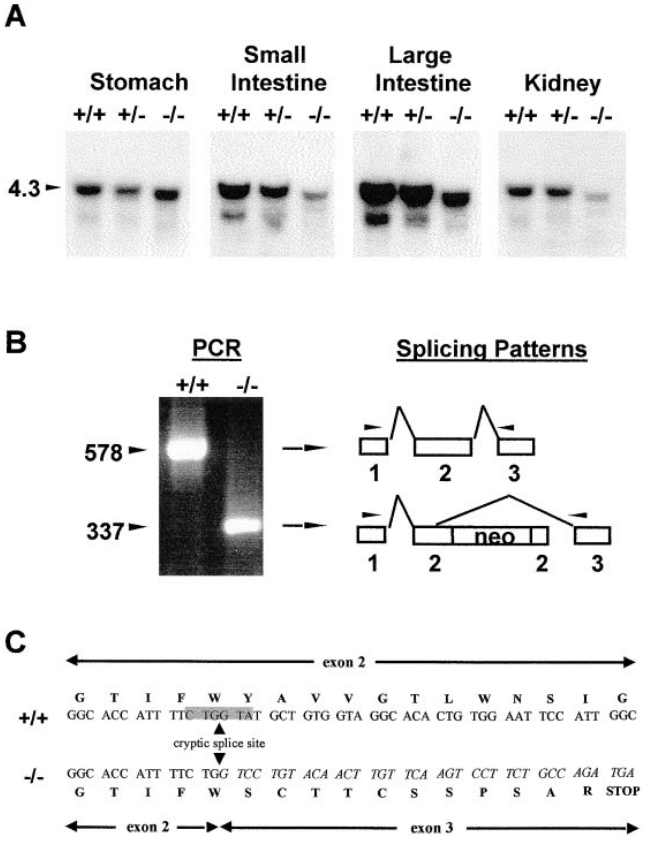

Figure 2. Northern blot analysis and characterization of mutant mRNA transcripts. (*A*) Northern blot analysis of total RNA (10 μg) isolated from the indicated tissues of adult animals. The blot was hybridized with a rat NHE2 cDNA probe, and the autoradiographic exposure time was 3 d. (*B*) RT-PCR analysis of wild-type and mutant mRNAs. RNA from *NHE2*$^{+/+}$ and *NHE2*$^{-/-}$ stomachs was reverse transcribed using an NHE2-specific primer. PCR amplification of wild-type and homozygous mutant first strand cDNAs using specific primers (*arrowheads*) from exons 1 and 3 yielded PCR products of 578 (wild-type) and 337 (mutant) bp, which correspond to the splicing patterns for exons 1, 2, and 3 (*right*). (*C*) Sequence analysis of the PCR products demonstrated that a cryptic donor splice site in exon 2 of the mutant gene was spliced to the acceptor site of exon 3. The nucleotide and deduced amino acid sequence of the region containing the cryptic splice is shown. Note that the aberrant splice causes a deletion, a frameshift (denoted by nucleotides in italics), and the introduction of a stop codon.

served for 355 pups from heterozygous matings. These data indicated that there is little, if any, embryonic or fetal lethality among the *NHE2*$^{-/-}$ mice. The *NHE2*$^{-/-}$ mice survived, grew normally, and were indistinguishable from *NHE2*$^{+/+}$ mice in their outward appearance and behavior. Homozygous mutant mating pairs yielded occasional litters, but in general they did not breed well. The basis for the poor breeding is not known and is being investigated.

Systemic acid-base and electrolyte status. To determine whether the absence of NHE2 in kidney and/or intestine might cause disturbances of acid-base or sodium homeostasis, we analyzed blood gases, pH, HCO_3^-, and electrolyte concentrations and determined plasma aldosterone levels in mice maintained under normal conditions. As shown in Table I, blood pH, HCO_3^-, and Na^+ concentrations and plasma aldosterone levels were virtually identical in the two groups, indicating that the lack of NHE2 caused no significant perturbations of acid-base or sodium homeostasis.

Pathological survey. A survey was performed on those epithelial tissues (stomach, intestine, and kidney) in which NHE2 is predominantly expressed. Despite the high levels of NHE2 expression in small intestine, cecum, colon, and kidney of wild-type mice, no significant histopathology was observed in these tissues of *NHE2*$^{-/-}$ mice. Also, gross inspection of the intestinal tract revealed no evidence of excess fluid accumulation that would be indicative of a defect in Na^+ absorption.[2] The stomachs of *NHE2*$^{+/-}$ mice (data not shown) resembled those of wild-type mice, but severe abnormalities were observed in the gastric mucosa of the *NHE2*$^{-/-}$ mice.

Structural abnormalities in the oxyntic mucosa of the gastric corpus. As shown in toluidine blue–stained semithin sections (Fig. 3), there were major alterations of the oxyntic mucosa of *NHE2*$^{-/-}$ mice. Severe histopathology was observed in the corpus of both adult (Fig. 3 *B*) and 17-d-old (Fig. 3 *C*) null mutants. Total counts of cells from the neck to the base of the gastric units demonstrated that parietal cell numbers were reduced sharply in stomachs of both young and adult *NHE2*$^{-/-}$ animals relative to controls (see Fig. 3, and Table II). 36.4±3.3% of the cells counted in the glandular epithelium of wild-type mice were parietal cells, compared with 5.0±2.4% in *NHE2*$^{-/-}$ animals (Table II). Among the reduced numbers of parietal cells in both young and adult null mutants, there were a few mature, normal-appearing parietal cells, but most were altered morphologically (Fig. 3, *B* and *C*) relative to wild-type cells (Fig. 3 *A*). Some of the altered parietal cells appeared to be in a state of active acid secretion, while others were immature or were vacuolated. There was also an increase in the number of parietal cells that appeared to be necrotic (Table II, and Fig. 3), and remnants of dead parietal cells were observed frequently in the dilated lumina of *NHE2*$^{-/-}$ gastric glands.

2. In contrast to the results with the NHE2 null mice, a severe absortive defect is observed in the intestine of homozygous NHE3 null mice (P.J. Schultheis and G.E. Shull, unpublished observations).

Table I. Blood Gases, Plasma Electrolytes, and Serum Aldosterone

	pH	HCO_3^-	Na^+	K^+	Cl^-	pCO_2	pO_2	Aldosterone*
	pH U	*mM*	*mM*	*mM*	*mM*	*mmHg*	*mmHg*	*ng/ml*
+/+	7.39±0.03	23.0±1.0	151.3±1.8	6.2±0.51	119.8±3.3	39.1±0.8	76.9±1.1	1.03±0.28
−/−	7.43±0.01	24.3±1.1	151.1±1.0	7.0±0.25	123.3±1.3	37.6±1.5	73.5±2.1	0.95±0.12

Values are means±SEM for four *NHE2*$^{+/+}$ and seven *NHE2*$^{-/-}$ samples. *Values are means±SEM for seven *NHE2*$^{+/+}$ and nine *NHE2*$^{-/-}$ samples.

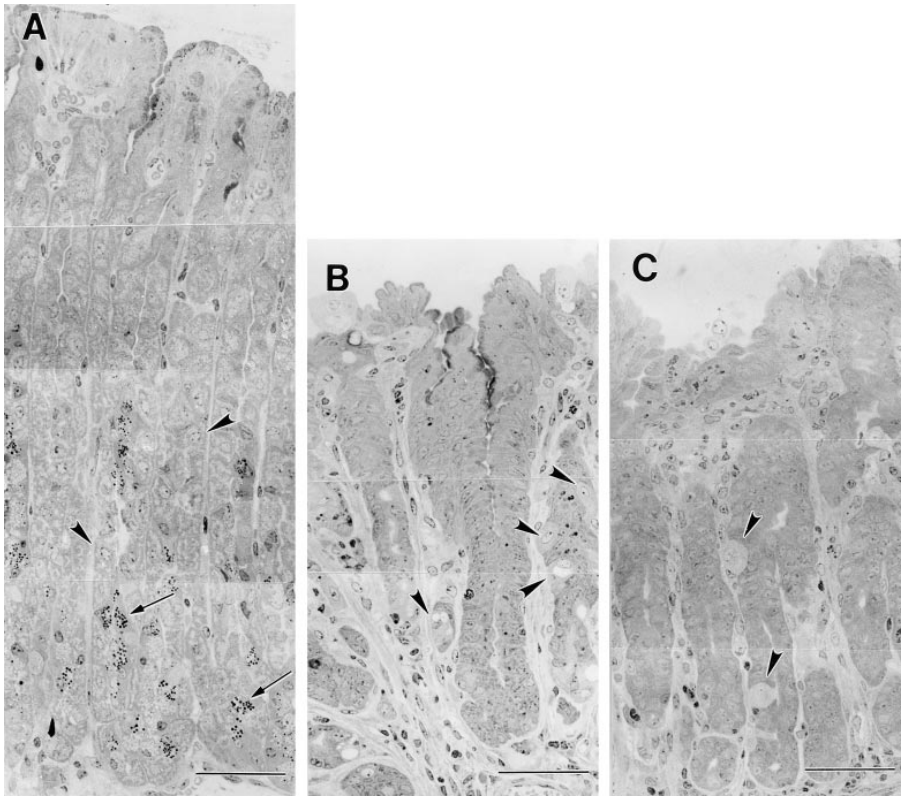

Figure 3. Toluidine blue–stained sections of gastric glands in the corpus of adult $NHE2^{+/+}$ (*A*) and $NHE2^{-/-}$ mice (*B*), and from a 17-d-old $NHE2^{-/-}$ mouse (*C*). (*A*) Differentiated parietal cells (*arrowheads*) with characteristic mottled appearance and mature zymogenic cells (*arrows*) with numerous dense secretory granules are apparent in the normal gastric glands. (*B*) In the adult $NHE2^{-/-}$ mice, mature zymogenic cells are absent, and the number of parietal cells are sharply reduced. Some parietal cells (*arrowheads*) contain large vacuoles and appear to be in various states of degeneration (the two lower cells indicated), whereas others (the two upper cells indicated) have abnormally light-staining cytoplasm. Note the structural changes characterized by expansion of the lamina propria, reduction in the volume of the gastric glands, and the presence of inflammatory cells. (*C*) Fewer of the parietal cells (*arrowheads*) in the 17-d-old $NHE2^{-/-}$ mice appear vacuolated compared with adult mutant animals, but they do have the abnormally light-staining cytoplasm. Scale bar, 50 μm.

The mean mucosal thickness on the greater curvature of the stomach was decreased by ~ 15% in $NHE2^{-/-}$ stomachs relative to wild-type mice (Table II). Despite the decrease in thickness, the stomachs of adult $NHE2^{-/-}$ mice were enlarged and weighed more than those of heterozygous and wild-type animals when normalized to body weight ($NHE2^{+/+}$, 5.9±0.2; $NHE2^{+/-}$, 6.0±0.2; $NHE2^{-/-}$, 7.0±0.3 mg/g body wt; $n = 17$ for each genotype; $P < 0.01$). The lamina propria at the base of the gastric units as well as that projecting between the units was thickened and contained numerous inflammatory cells, including neutrophils, eosinophils, lymphocytes, and plasma cells. Numerous tissue basophil-like cells lay against the basement membrane of the gastric glands in the $NHE2^{-/-}$ mice. Hyperplasia in the mucosa of the gastric corpus was seen in $NHE2^{-/-}$ mice, and the glandular mitotic index (Table II) was elevated significantly in null mutants.

Table II. Comparison of Epithelial Cell Populations in the Corpus of $NHE2^{+/+}$ and $NHE2^{-/-}$ Stomachs

Cell type	+/+	−/−	
Parietal	36.4±3.3	5.0±2.4	($P = 0.0001$)
Zymogen	17.3±2.2	2.5±1.5	($P = 0.0001$)
Enterodendocrine	1.0±0.3	0.7±0.2	($P = 0.42$)
Eosinophilic cells*	0.06±0.03	1.0±0.3	($P = 0.0031$)
Necrotic parietal	0.02±0.02	0.4±0.1	($P = 0.0038$)
Mitosis	0.35±0.07	1.5±0.3	($P = 0.0016$)
Other‡	44.9±4.4	89.9±3.4	($P = 0.0001$)
Glandular thickness (μm)*	363.5±18.8	308.2±20.6	($P = 0.059$)

Data are derived from toluidine blue–stained plastic sections unless noted otherwise. Values for each cell type are the means±SEM and represent the percentage of the total epithelial cell population, $n = 7$ for each genotype. *Data derived from hematoxylin and eosin–stained paraffin sections, $n = 13$ for each genotype. ‡Mucous cells with granules and all other nondifferentiated cell-types.

The zymogenic (chief) cell population was reduced in $NHE2^{-/-}$ mice, and mature zymogenic cells were rare (Fig. 3), consistent with a block in maturation. Zymogenic cells comprised 17.3±2.2% of the cells in the corpus of $NHE2^{+/+}$ mice and 2.5±2.2% of those in $NHE2^{-/-}$ mice (Table II). Enteroendocrine cells were present in roughly equivalent numbers in the wild-type and $NHE2^{-/-}$ mice. Mucous cells and cells that were relatively undifferentiated represented an increased proportion of the gastric unit in $NHE2^{-/-}$ mice.

No histopathology was observed in the forestomach of $NHE2^{-/-}$ mice, and the only histological change observed in the antrum was hyperplasia of mucous cells (data not shown), which occurred in adult but not juvenile $NHE2^{-/-}$ mice. This hyperplasia may be secondary to the increased serum gastrin concentrations discussed below. There was no apparent increase in the incidence of cell death in forestomach or antrum.

Ultrastructure of gastric parietal cells. By light microscopy at high magnification, normal parietal cells appear as large, lightly staining pyramid-shaped cells with many mitochondria scattered throughout the cytoplasm, which gives them a characteristic mottled appearance (Fig. 3 *A*). The mutant parietal cells were frequently misshapen and vacuolated (such as the two lower cells labeled in Fig. 3 *B*), and often appeared as large cells with a uniformly light-staining cytoplasm (such as

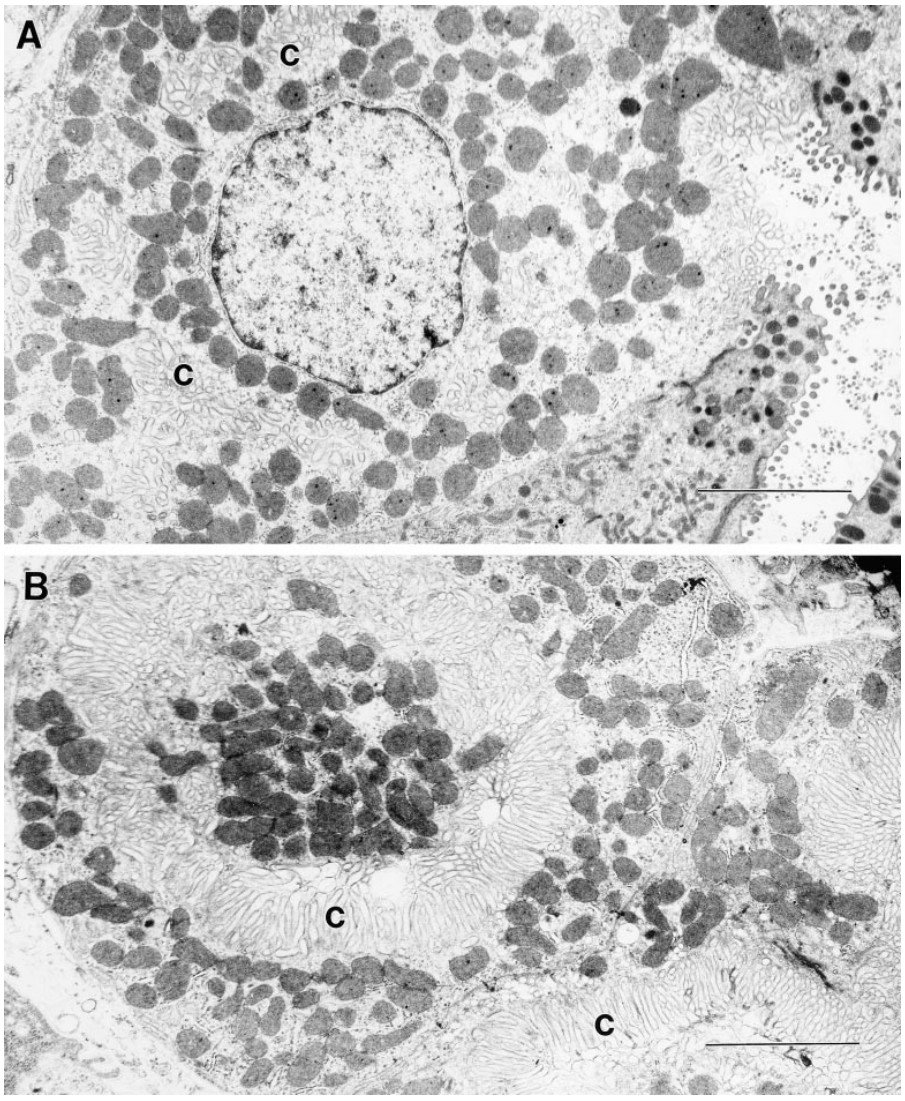

Figure 4. Electron micrographs of parietal cells from 6-mo-old $NHE2^{+/+}$ (*A*) and $NHE2^{-/-}$ (*B*) mice. These cells have numerous mitochondria and extensive intracellular canalicular systems (*c*). The mutant parietal cell has many long microvilli and is virtually devoid of tubulovesicular membranes. Both features are characteristic of parietal cells that are secreting acid at a high rate. Scale bar, 5 μm.

the two upper cells labeled in Fig. 3 *B* and those labeled in Fig. 3 *C*), rather than having the mottled appearance of wild-type cells. To determine the basis for these alterations in parietal cell morphology, electron microscopy was performed.

Parietal cells from $NHE2^{-/-}$ mice appear either to be immature, mature and actively secreting, or to be in various stages of degeneration. The number of immature and degenerating parietal cells exceeded the number of mature, actively secreting cells. Parietal cells that appear to be engaged in acid secretion, from 6-mo-old wild-type and homozygous mutant mice, are shown in Fig. 4. The wild-type cell (Fig. 4 *A*) has well-formed secretory canaliculi that are characteristic of mature parietal cells. The mature parietal cells from $NHE2^{-/-}$ mice were filled with an increased quantity of canalicular membranes (Fig. 4 *B*), indicating that they are engaged in high levels of acid secretion. The mutant parietal cells shown in Fig. 4 *B* seem to correspond in appearance to the morphologically altered parietal cells, with uniformly light-staining cytoplasm that are labeled with arrowheads in Fig. 3 *C* (from 17-d-old $NHE2^{-/-}$ mice). Similar parietal cells can also be observed in sections from an adult $NHE2^{-/-}$ animal shown in Fig. 3 *B*.

While some of the parietal cells seen in the gastric units of both young and adult $NHE2^{-/-}$ mice appear viable, in others the tubulovesicular system has collapsed, and large cytoplasmic vacuoles and distended canaliculi (Fig. 5), indicative of a loss of viability, are observed. These parietal cells, from both adult (Fig. 5 *A*) and 19-d-old (Fig. 5 *B*) mutants, seem to correspond to the vacuolated parietal cells labeled in Fig. 3 *B*. Altered parietal cells such as these have been observed previously in the gastric units of wild-type mice (19); however, they occur in much greater numbers in the gastric glands of $NHE2^{-/-}$ mice than in the glands of wild-type mice.

TUNEL assays of gastric sections. The ultrastructural analyses suggested that parietal cell death in $NHE2^{-/-}$ stomachs occurred primarily by necrosis. To further evaluate the mechanism of cell death, we performed TUNEL assays, which detect the DNA fragmentation that occurs during the initial stages of apoptotic cell death. As shown in Fig. 6 *A*, TUNEL-positive cells, indicated by nuclear staining, are uncommon in the corpus of wild-type mice, with most staining observed in surface cells, and only occasional staining observed deeper in the glands. In the corpus of $NHE2^{-/-}$ mice, there was a slight in-

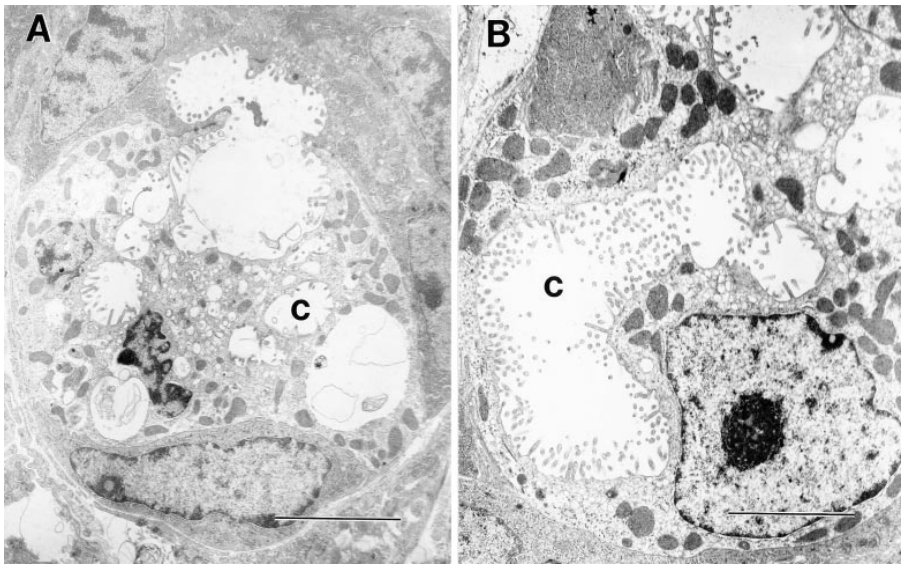

Figure 5. Electron micrographs of degenerating parietal cells from 6-mo-old (*A*) and 19-d-old (*B*) *NHE2*$^{-/-}$ mice. The cells have numerous mitochondria which are primarily confined to the cell periphery, and abormally distended canaliculi (*c*). These cells are similar in appearance to the vacuolated parietal cells observed in toluidine blue–stained sections in Fig. 3 *B*. Scale bar, 5 μm.

crease in the number of TUNEL-positive cells in the surface epithelium (Fig. 6 *B*), but staining in deeper segments of the gland was rare.

Decreased H$^+$*,K*$^+$*-ATPase and pepsinogen mRNA and increased gastrin mRNA and serum gastrin.* The histological studies revealed a sharp reduction in the number of parietal and zymogenic cells. To confirm the severity of this decrease, Northern blot analysis of RNA from the stomachs of *NHE2*$^{+/+}$ and *NHE2*$^{-/-}$ mice was performed using hybridization probes specific for the gastric H$^+$,K$^+$-ATPase α-subunit mRNA, which is restricted to parietal cells, and pepsinogen mRNA, which is restricted to zymogenic cells. As shown in Fig. 7, there was a sharp decrease in the expression of these genes in the mutant animals. The decrease in levels of these mRNAs seemed to exceed the magnitude of the observed reduction in the two cell populations, possibly reflecting the relative immaturity and apparently reduced viability of the parietal cells and the immaturity of the zymogenic cells in *NHE2*$^{-/-}$ mice.

The peptide hormone gastrin, produced by G cells of the antral mucosa, regulates acid secretion and exerts a trophic effect on the gastric mucosa (20). Therefore, it was of interest to determine whether ablation of the NHE2 gene leads to an alteration of gastrin mRNA levels and serum gastrin concentrations. Northern blot analysis of stomach RNA using a gastrin cDNA probe and RIA of serum gastrin levels demonstrates that both gastrin mRNA (Fig. 8 *A*) and serum gastrin concentrations (Fig. 8 *B*) were elevated in the *NHE2*$^{-/-}$ mice. These results indicate that G cells are present and functional in the stomachs of mutant mice, and that increased gastrin synthesis is occurring in response to the alterations in the gastric mucosa.

Loss of net acid secretion in adult null mutants. To determine whether the observed reduction in the number of parietal cells causes a corresponding decrease in acid secretion, the pH and acid-base content of gastric secretions were measured in both mutant and wild-type animals. In the initial study (Fig. 9 *A*),

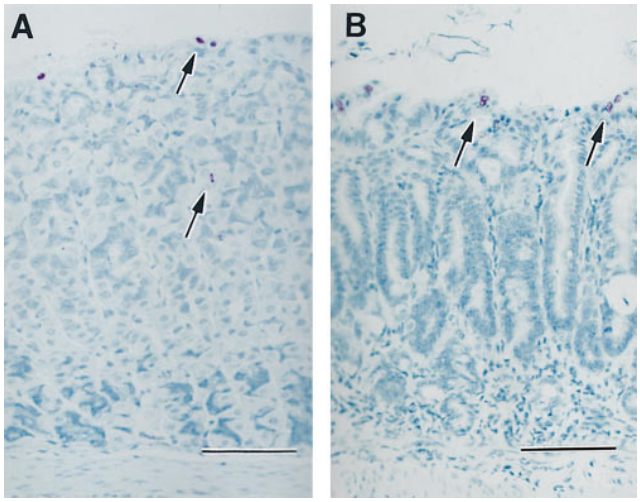

Figure 6. Detection of apoptotic cells in corpus of wild-type (*A*) and NHE2-deficient (*B*) mice. TUNEL-positive cells (*purple, arrows*) in stomachs of both wild-type and mutant mice were detected primarily among the surface cells, with occasional staining observed deeper in the glands (*lower arrow* in *A*). The frequency of TUNEL-positive cells in the surface epithelium of *NHE2*$^{-/-}$ stomachs was slightly greater than in wild-type stomachs, but no increase was observed in deeper segments of the gland where degenerating parietal cells were observed. Scale bar, 100 μm.

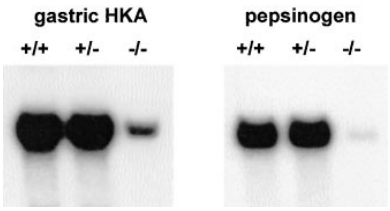

Figure 7. Northern blot analysis of gastric H$^+$,K$^+$-ATPase and pepsinogen mRNA in stomach. Each lane contains 10 μg of total RNA from 9-wk-old wild-type (+/+), heterozygous (+/−), and homozygous mutant (−/−) mice, which was hybridized with rat gastric H$^+$,K$^+$-ATPase (HKA) or rat pepsinogen cDNA probes. Autoradiographic exposure times were 24 h for the H$^+$,K$^+$-ATPase analysis and 11 min for the pepsinogen analysis.

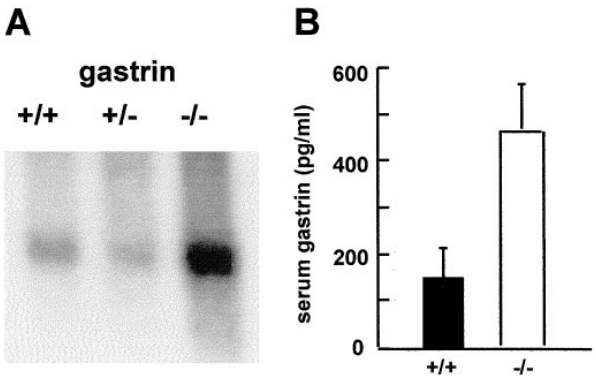

Figure 8. Gastrin mRNA in stomach and serum gastrin levels. (*A*) Northern blot analysis of total RNA (10 μg per lane) from 9-wk-old wild-type (+/+), heterozygous (+/−), and homozygous mutant (−/−) stomachs using a mouse gastrin cDNA probe. The autoradiograph was exposed for 21 h. (*B*) Serum gastrin concentrations in 8-wk-old $NHE2^{+/+}$ and $NHE2^{-/-}$ mice were measured by RIA. *Error bars*, SEM for serum samples from seven wild-type and nine mutant animals. The average wild-type and mutant serum gastrin concentrations were 149±62 and 464±95 pg/ml, respectively. $P = 0.02$ as determined by single-factor ANOVA.

using adult animals treated with histamine to stimulate acid secretion, the pH of gastric secretions ranged from 7.28 to 8.91 in $NHE2^{-/-}$ animals (7.82±0.11), from 2.35 to 4.10 in $NHE2^{+/-}$ mice (3.02±0.18), and from 2.43 to 4.24 in $NHE2^{+/-}$ mice (3.21±0.16). To quantify the net amount of acid or base in the stomachs of these same adult animals, the gastric contents of the animals were titrated to pH 6.5 with NaOH or HCl (Fig. 9 *B*). The amount of acid ranged from 9.1 to 99.6 μeq/g wet wt in $NHE2^{+/+}$ animals (45.0±7.0), and from 12.0 to 131.7 in $NHE2^{+/-}$ mice (52.7±4.0). In contrast, gastric contents in age-matched homozygous mutants were basic. The amount of base ranged from 8.1 to 68.7 μeq/g wet wt in stomachs of $NHE2^{-/-}$ mice (18.5±11.0).

Because the number of parietal cells was also reduced in 17-d-old null mutants (Figs. 3 and 4), we performed an additional experiment to determine whether net acid secretion is also absent in $NHE2^{-/-}$ mice just before weaning. In contrast to adult $NHE2^{-/-}$ mice, 18–19-d-old $NHE2^{-/-}$ mice do maintain net secretion of gastric acid (Fig. 9 *C*), although the levels of acid secretion are slightly lower than in $NHE2^{+/+}$ mice. The pH of gastric secretions of the 18–19-d-old $NHE2^{-/-}$ mice ranged from 3.17 to 5.06 (4.13±0.25), whereas the pH of gastric secretions of age-matched $NHE2^{+/+}$ controls ranged from 3.07 to 4.10 (3.57±0.12). After determining that net acid secretion was present in mice before weaning, a small set of juvenile animals was also analyzed (Fig. 7 *C*). The pH of gastric secretions of 45-d-old $NHE2^{-/-}$ mice ranged from 5.1 to 7.8 (6.26±0.55), whereas the pH of gastric secretions of age-matched $NHE2^{+/+}$ controls ranged from 2.24 to 3.16 (2.81±0.15).

Discussion

Preparation and phenotype of NHE2-deficient mouse. To develop the mouse model, we used ES cell technology to disrupt exon 2 of the NHE2 gene. PCR analysis of the mutant mRNA demonstrated that it had a deletion and a frameshift in the coding sequence that eliminated nine of the putative transmembrane domains, which are essential for Na^+/H^+ exchange activity (21). The mutant mice were born in the normal Mendelian ratios and were indistinguishable from wild-type animals in their appearance and behavior. Despite the high levels of NHE2 mRNA expression in mouse kidney and intestine, we

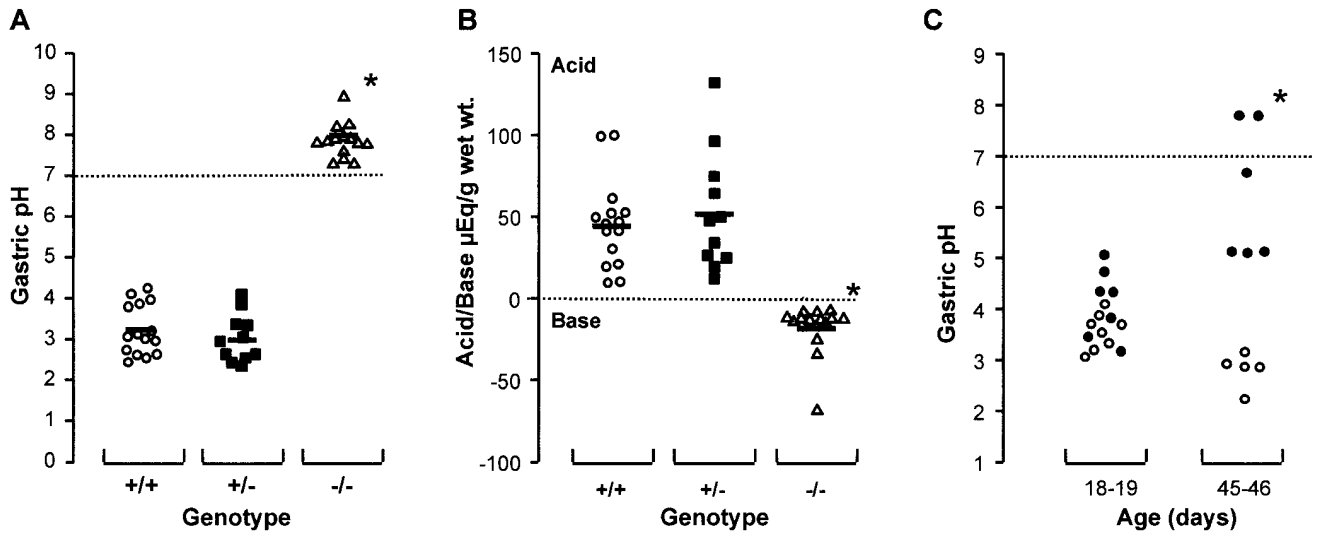

Figure 9. Gastric acid secretion in $NHE2^{+/+}$, $NHE2^{+/-}$, and $NHE2^{-/-}$ mice. All measurements of stomach contents were made 15 min after subcutaneous injection of histamine HCl (2 μg/g body wt). (*A*) pH of gastric secretions, and (*B*) acid-base content of gastric secretions in adult mice. Total acid and base equivalents were determined by titration with either 0.01 N NaOH or HCl. Data were normalized to the blotted wet weight of the stomach. *Horizonal bars* in *A* and *B* represent mean values of data for each genotype. $n = 15$ (+/+), 11 (+/−), and 15 (−/−). *Significantly different from $NHE2^{+/+}$ and $NHE2^{+/-}$ mice by ANOVA-protected Bonferroni's *t* test ($P < 0.00001$). There was no significant difference in values for $NHE2^{+/+}$ and $NHE2^{+/-}$ mice. (*C*) Age dependence of acid secretion. *Open circles*, $NHE2^{+/+}$; *filled circles*, $NHE2^{-/-}$. $n = 8$ (+/+) and 7 (−/−) for 18–19-d-old mice; $n = 5$ (+/+) and 6 (−/−) for 45-d-old mice. $P = 0.059$ for difference between 18-d-old $NHE2^{+/+}$ and $NHE2^{-/-}$ mice, $P < 0.001$ for difference between 45-d-old $NHE2^{+/+}$ and $NHE2^{-/-}$ mice.

observed no physiological perturbations that could be attributed to altered renal or intestinal function. There were no apparent differences in blood pH, HCO_3^-, Na^+, or aldosterone levels between *NHE2*$^{-/-}$ and *NHE2*$^{+/+}$ mice, and there was no indication of an absorptive defect in the intestine.[2] However, in stomach there was a sharp reduction in the number of gastric parietal and zymogenic cells, and there was a loss of net acid secretion in adult but not juvenile mice. The histopathology observed in the gastric mucosa of NHE2-deficient mice and the loss of net acid secretion demonstrated that NHE2 plays a critical role in gastric mucosal function. These results are in sharp contrast to those reported for NHE1-deficient mice, in which gastric mucosal abnormalities were not observed (22).

The occurrence of net acid secretion in young null mutants (Fig. 9) and the presence of apparently functional parietal cells in adult mutants (Fig. 4 *B*) indicated that the lack of NHE2 does not prevent the generation or maturation of parietal cells, although some interference in these processes cannot be ruled out. However, the viability of NHE2-deficient parietal cells appeared to be sharply reduced. Diminished viability rather than a block in their development was indicated by the altered appearance of most of the parietal cells, including those that appeared functional. For example, the mutant parietal cells shown in Fig. 4 *B*, which appeared to be secreting acid at a high rate, showed some indications that vacuoles were beginning to form, and some collapse of the tubulovesicular system seemed to be occurring in the cell in the lower right of Fig. 4 *B*. Despite the overall reduction in the number of parietal cells in NHE2-deficient animals, there was a sharp increase in the numbers of vacuolated, degenerating, and necrotic parietal cells. These data indicated that *NHE2*$^{-/-}$ parietal cells are able to develop and begin secreting acid but then degenerate rapidly.

Previous work has shown that in the normal mouse stomach, parietal cells die by both necrosis and apoptosis (19). Necrotic parietal cells are generally extruded into the lumen of the gland or into the gastric lumen, whereas apoptotic parietal cells are phagocytosed by macrophages, zymogenic cells, or mucous cells (19). On the basis of ultrastructural analyses, necrosis appeared to be the primary mode of parietal cell death in the *NHE2*$^{-/-}$ stomachs. The marked increase in the number of inflammatory cells and the frequent occurrence of parietal cell remnants in the lumina of the gastric glands of *NHE2*$^{-/-}$ stomachs was consistent with this conclusion. Although TUNEL assays (Fig. 6) revealed that *NHE2*$^{-/-}$ stomachs had a slight increase in the number of surface cells exhibiting DNA fragmentation, which occurs during the early stages of apoptosis (23), the virtual absence of TUNEL-positive cells within the deeper segments of the glands further supported the conclusion that the lack of NHE2 leads to necrotic, rather than apoptotic death of parietal cells.

Data from previous studies (4, 5) strongly suggested that basolateral Na^+/H^+ exchange is the major mechanism for protecting zymogenic cells from acid stress. In *NHE2*$^{-/-}$ stomachs, mature zymogenic cells were rarely observed, and the numbers of zymogenic cells were sharply reduced. Although these data are consistent with the possibility that NHE2 might be required for zymogenic cell differentiation, firm conclusions regarding the role of NHE2 in zymogenic cells cannot be drawn from these results, as either the loss of parietal cells (24, 25) or the inhibition of acid secretion (26) causes a block in the maturation of zymogenic cells. Thus, the effects of the NHE2 null mutation on zymogenic cells may be secondary to the reduced viability of parietal cells.

Unique characteristics of NHE2 and possible relationship to gastric mucosal function. The membrane location of NHE2 varies depending on the cell type. It is expressed on the basolateral membranes of renal medullary collecting duct cells (27) and on brush border membranes in the intestine (28). Because NHE2 is coexpressed with NHE1 and NHE4 in all three of the major epithelial cell types in gastric mucosa (8), it presumably mediates some of the Na^+/H^+ exchange activity that has been identified on the basolateral membranes of parietal (1, 2, 4, 5, 7), zymogenic (4, 5), and mucous cells (5, 6). The precise physiological functions of individual isoforms are unclear, but it seems likely that differences in their functional characteristics enable each isoform to respond differently to varying signals and conditions in the gastric mucosa.

An unusual biochemical characteristic of NHE2 is that it is highly sensitive to inhibition by extracellular H^+. It is strongly upregulated by extracellular alkalinity (13), with half-maximal activity at pH 8 and full activity at pH 9. Therefore, its activity would be expected to increase in response to the increased interstitial HCO_3^- that occurs during secretion of acid. This unique property correlates well with the observation of Seidler et al. (7) that an NHE on the basolateral membrane of the gastric parietal cell is upregulated in response to increased serosal HCO_3^- and pH , a response that the authors attributed to "disinhibition" of Na^+/H^+ exchange. Upregulation of its activity during acid secretion might allow NHE2 to function as an important component of the basolateral transport processes needed for high rates of acid secretion by the parietal cell and/or for the maintenance of parietal cell viability. In addition, increased activity of NHE2 in the basolateral membrane of chief and mucous cells in response to increased interstitial alkalinity might allow this isoform to play a major role in mucosal protection.

Possible functions of NHE2 in the parietal cell. As a test of the hypothesis that NHE2 is required for maximum acid secretion, we compared gastric acid secretion in stomachs of *NHE2*$^{+/+}$ mice with that of both heterozygous and homozygous mutants (Fig. 9). A reduction in gastric acid secretion in the stomachs of NHE2 heterozygous mutants, in which NHE2 mRNA levels were reduced, would have indicated that NHE2 activity is rate-limiting for acid secretion; however, this reduction did not occur. Net acid secretion was reduced in *NHE2*$^{-/-}$ mice just before weaning and was absent in adult *NHE2*$^{-/-}$ mice, but this was probably due to the loss of parietal cells rather than reduced acid secretion by individual parietal cells, as the pH of stomach contents from 18–19-d-old null mutants was only slightly higher than that of wild-type mice, suggesting that the remaining parietal cells were secreting acid at a high rate. In addition, some of the parietal cells observed in both young and adult null mutants (see Fig. 3, *B* and *C*, and Fig. 4 *B*) appeared to be in a state of hypersecretion, as their cytoplasmic spaces were filled with massive quantities of canalicular membranes. Thus, the results of our analyses of acid secretion, histopathology of the gastric mucosa, and ultrastructure of the parietal cell in NHE2$^{+/+}$, NHE2$^{+/-}$, and NHE2$^{-/-}$ mice indicated that NHE2 is not required to achieve high levels of acid secretion by individual parietal cells.

A second hypothesis for the physiological role of NHE2 in the parietal cell is that it functions as a component of the basolateral transport mechanisms that maintain cellular homeosta-

sis. During acid secretion the basolateral transporters must maintain an intracellular milieu that is appropriate for both acid secretion and long-term viability of the parietal cell. Given the massive fluxes of H^+, HCO_3^-, electrolytes, and fluid that occur during acid secretion, maintaining homeostasis of the parietal cell during its 54–d life span (19) is a formidable task. How might the parietal cell meet this challenge? One means of doing this would be to have an array of transporters on the basolateral membrane working both separately and in concert, each having characteristics that allow it to respond to perturbations in a manner that tends to restore cellular homeostasis. The stimulated parietal cell must have highly efficient mechanisms for maintenance of volume homeostasis. Cell volume depletion due to the secretion of large quantities of an isotonic solution of H^+, K^+, and Cl^- across the apical membrane must be counteracted by electrolyte and fluid uptake across the basolateral membrane. All three of the NHEs expressed in the parietal cell (29–31) and the AE2 Cl^-/HCO_3^- exchanger (32) are stimulated by cell shrinkage. By responding to cell shrinkage with increased transport activity, thereby increasing the rate of electrolyte and water entry across the basolateral membrane, the cell would replace the ions and water being secreted across the apical membrane, dispose of excess HCO_3^- being generated, and maintain its membrane potential. However, response to cell volume-depletion is unlikely to be the only mechanism for upregulation of the basolateral transporters that replace the ions and water being secreted, as the volume depleted state might not be fully compatible with long-term viability.

The previously observed induction of an NHE on the basolateral membrane of the parietal cell in response to increased extracellular pH and HCO_3^- (7), and the demonstrated upregulation of NHE2 activity in response to an increase in extracellular alkalinity (13), suggests that NHE2 is regulated coordinately with acid secretion. For the following reasons, this might enable NHE2 to play a major role in maintaining the viability of the parietal cell. Under resting conditions, when the need for electrolyte entry across the basolateral membrane is minimal and interstitial pH and HCO_3^- concentrations are low, NHE2 should be relatively inactive. However, when acid secretion is stimulated and HCO_3^- is extruded across the basolateral membrane, then the resulting increase in alkalinity should relieve the inhibition of NHE2 by extracellular H^+ (the "disinhibition" noted by Seidler et al. [7]). This in turn might allow NHE2, in concert with the NHE1 and NHE4 NHEs, one or more variants (33) of the AE2 Cl^-/HCO_3^- exchanger (34), the Na^+,K^+-ATPase, and possibly the basolateral Na^+,K^+,$2Cl^-$ cotransporter (35), which is also upregulated by cell volume depletion (36), to mediate the electrolyte uptake needed to maintain optimum conditions for both acid secretion and long-term viability of the parietal cell. However, in the NHE2-deficient mouse, this auxiliary Na^+/H^+ exchange activity, which may normally be upregulated during acid secretion, is absent. Nevertheless, acid secretion does occur, apparently even in parietal cells of 6-mo-old *NHE2*$^{-/-}$ mice judging from the massive secretory canaliculi observed in mutant parietal cells (Fig. 4 *B*), demonstrating that the remaining basolateral transport mechanisms are sufficient to maintain acid secretion. However, the data strongly indicate that the viability of the parietal cell is sharply reduced. The underlying mechanism by which the ablation of NHE2 decreases parietal cell viability is unclear, but one possibility is that volume homeostasis is severely perturbed. Even though the NHE2-deficient parietal cell is capable of maintaining high rates of acid secretion during its brief life span, the ATP-dependent secretion of acid, with accompanying electrolytes and water across the apical membrane, might place the cell in a chronically volume-depleted state that is incompatible with long-term viability.

Possible functions of NHE2 in mucosal protection. Upregulation of NHE2 in response to a rise in extracellular alkalinity could enable this isoform to function in mucosal protection in the classical sense of protecting the epithelial cells from acid damage. Na^+/H^+ exchange on the basolateral membrane of zymogenic cells and mucous cells, in which NHE2 is expressed, protects these cells by extruding H^+ that diffuses into the cytoplasm. It has long been known that the gastric mucosa is more resistant to luminal acid when the parietal cell is actively secreting (37–39), and it is clear that interstitial HCO_3^-, produced by the stimulated parietal cell is largely responsible for the increased protection (for a review, see reference 40). Studies of the microvasculature of rat (41) and human (42) stomach led Gannon and colleagues to propose that during gastric acid secretion, HCO_3^- secreted across the basolateral membrane of the parietal cell is transported efficiently to the basal side of surface epithelial cells, and enables these cells to either dispose of H^+ leaking into the cell or secrete HCO_3^- into the lumen. The mechanism by which mucous cells respond to increased interstitial HCO_3^- has not been determined, but an attractive possibility is that this response is mediated by NHE2. As discussed above, the extracellular pH sensitivity of NHE2 would allow this exchanger to increase its activity in response to the increased interstitial HCO_3^- that occurs during acid secretion. We did not observe evidence of acid damage to mucous cells; however, the data obtained in this study cannot address adequately the issue of whether NHE2 protects mucous cells from acid stress because net acid secretion is lost rapidly due to the reduced viability of parietal cells. To determine whether NHE2 functions in mucosal protection, it may be necessary to develop an animal model in which conventional transgenesis is used to restore the expression of NHE2 specifically in parietal cells of the NHE2-deficient mouse.

Acknowledgments

We thank Stacey Andringa and Jeannette Greeb for expert technical assistance.

This work was supported by National Institutes of Health grants DK-50594, HL-41496, DK-39626, and DK-48816.

References

1. Muallem, S., C. Burnham, D. Blissard, T. Berglindh, and G. Sachs. 1988. Electrolyte transport across the basolateral membrane of the parietal cells. *J. Biol. Chem.* 260:6641–6653.

2. Muallem, S., D. Blissard, E.J. Cragoe, Jr., and G. Sachs. 1988. Activation of the Na^+/H^+ and Cl^-/HCO_3^- exchange by stimulation of acid secretion in the parietal cell. *J. Biol. Chem.* 263:14703–14711.

3. Paradiso, A.M., P.A. Negulescu, and T.E. Machen. 1986. Na^+-H^+ and Cl^--OH^-(HCO_3^-) exchange in gastric glands. *Am. J. Physiol.* 250:G524–G534.

4. Paradiso, A.M., R.Y. Tsien, and T.E. Machen. 1987. Digital image processing of intracellular pH in gastric oxyntic and chief cells. *Nature.* 325:447–450.

5. Seidler, U., K. Carter, S. Ito, and W. Silen. 1989. Effect of CO_2 on pH_i in rabbit parietal, chief, and surface cells. *Am. J. Physiol.* 256:G466–G475.

6. Kaneko, K., P.H. Guth, and J.D. Kaunitz. 1992. Na^+/H^+ exchange regulates intracellular pH of rat gastric surface cells in vivo. *Pfluegers Arch.* 421: 322–328.

7. Seidler, U., P. Stumpf, and M. Classen. 1995. Interstitial buffer capacity influences Na^+/H^+ exchange kinetics and oxyntic cell pH_i in intact frog gastric

mucosa. *Am. J. Physiol.* 268:G509–G504.

8. Seidler, B., H. Rossmann, A. Murray, J. Orlowski, C.-M. Tse, M. Donowitz, G. Shull, M. Gregor, and U. Seidler. 1997. Expression of the Na^+/H^+ exchanger isoform NHE1-4 mRNA in the different epithelial cell types of rat and rabbit gastric mucosa. *Gastroenterology.* 112:A285. (Abstr.)

9. Allen, A., G. Flemstrom, A. Garner, and E. Kivilaakso. 1993. Gastroduodenal mucosal protection. *Physiol. Rev.* 73:823–857.

10. Schade, C., G. Flemstrom, and L. Holm. 1994. Hydrogen ion concentration in the mucus layer on top of acid-stimulated and -inhibited rat gastric mucosa. *Gastroenterology.* 107:180–188.

11. Wang, Z., J. Orlowski, and G.E. Shull. 1993. Primary structure and functional expression of a novel gastrointestinal isoform of the rat Na/H exchanger. *J. Biol. Chem.* 268:11925–11928.

12. Tse, C.-M., S.A. Levine, C.H.C. Yun, M.H. Montrose, P.J. Little, J. Pouyssegur, and M. Donowitz. 1993. Cloning and expression of a rabbit cDNA encoding a serum-activated ethylisopropylamiloride-resistant epithelial Na^+/H^+ exchanger isoform (NHE-2). *J. Biol. Chem.* 268:11917–11924.

13. Yu, F.H., G.E. Shull, and J. Orlowski. 1993. Functional properties of the rat Na/H exchanger NHE-2 isoform expressed in Na/H exchanger-deficient chinese hamster ovary cells. *J. Biol. Chem.* 268:25536–25541.

14. Orlowski, J. 1993. Heterologous expression and functional properties of amiloride high affinity (NHE-1) and low affinity (NHE-3) isoforms of the rat Na/H exchanger. *J. Biol. Chem.* 268:16369–16377.

15. Glauser, M., P. Bauerfeind, W. Feil, M. Riegler, R. Fraser, and A.L. Blum. 1996. Metabolic base production and mucosal vulnerability during acid inhibition in a mammalian stomach *in vitro. Dig. Dis. Sci.* 41:964–971.

16. Church, G.M., and W. Gilbert. 1984. Genomic sequencing. *Proc. Natl. Acad. Sci. USA.* 81:1991–1995.

17. Stechschulte, D.J., Jr., D.C. Morris, R.L. Jilka, and K.N. Dileepan. 1990. Impaired gastric acid secretion in mast cell-deficient mice. *Am. J. Physiol.* 259: G41–G47.

18. Wood, L.R., and A. Dubois. 1983. Scanning electron microscopy of the stomach during modifications of acid secretion. *Am. J. Physiol.* 244:G475–G479.

19. Karam, S.M. 1993. Dynamics of epithelial cells in the corpus of the mouse stomach. IV. Bidirectional migration of parietal cells ending in their gradual degeneration and loss. *Anat. Rec.* 236:314–332.

20. Brand, S.J., and W.E. Schmidt. 1995. Gastrointestinal hormones. *In* Gastroenterology, second ed. T. Yamada, editor. J.B. Lippincott Company, Philadelphia. 25–71.

21. Wakabayashi, S., P. Fafournoux, C. Sardet, and J. Pouyssegur. 1992. The Na^+/H^+ antiporter cytoplasmic domain mediates growth factor signals and controls H^+-sensing. *Proc. Natl. Acad. Sci. USA.* 89:2424–2428.

22. Cox, G.A., C.M. Lutz, C.-L. Yang, D. Biemesderfer, R.T. Bronson, A. Fu, P.S. Aronson, J.L. Noebels, and W.N. Frankel. 1997. Sodium/hydrogen exchanger gene defect in slow-wave epilepsy mutant mice. *Cell.* 91:139–148.

23. Gavrieli, Y., Y. Sherman, and S.A. Ben-Sasson. 1992. Identification of programmed cell death via specific labeling of nuclear DNA fragmentation. *J. Cell Biol.* 119:493–501.

24. Li, Q., S.M Karam, and J.I. Gordon. 1996. Diptheria toxin-mediated ablation of parietal cells in the stomach of transgenic mice. *J. Biol. Chem.* 271: 3671–3676.

25. Li, Q., S.M. Karam, and J.I. Gordon. 1995. Simian virus 40 T antigen-induced amplification of pre-parietal cells in transgenic mice. Effects on other gastric epithelial cell lineages and evidence for a p53-independent apoptotic mechanism that operates in a committed progenitor. *J. Biol. Chem.* 271:3671–3676.

26. Karam, S.M., and J.G. Forte. 1994. Inhibiting gastric H^+-K^+-ATPase activity by omeprazole promotes degeneration and production of parietal cells. *Am. J. Physiol.* 266:G745–G758.

27. Soleimani, M., G. Singh, G.L. Bizal, S.R. Gullans, and J.A. McAteer. 1994. Na^+/H^+ exchanger isoforms NHE-2 and NHE-1 in inner medulary collecting duct cells. Expression, functional localization, and differential regulation. *J. Biol. Chem.* 269:27973–27978.

28. Hoogerwerf, W.A., S.C. Tsao, O. Devuyst, S.A. Levine, C.H.C. Yun, J.W. Yip, M.E. Cohen, P.D. Wilson, A.J. Lazenby, C.-M. Tse, and M. Donowitz. 1996. NHE2 and NHE3 are human and rabbit intestinal brush-border proteins. *Am. J. Physiol.* 270:G29–G41.

29. Krump, E., K. Nikitas, and S. Grinstein. 1997. Induction of tyrosine phosphorylation and Na^+/H^+ exchanger activation during shrinkage of human neutrophils. *J. Biol. Chem.* 272:17303–17311.

30. Kapus, A., S. Grinstein, S. Wasan, R. Kandasamy, and J. Orlowski. 1994. Functional characterization of three isoforms of the Na^+/H^+ exchanger stably expressed in chinese hamster ovary cells. ATP dependence, osmotic sensitivity, and role in cell proliferation. *J. Biol. Chem.* 269:23544–23552.

31. Bookstein, C., M.W. Musch, A. DePaoli, Y. Xie, M. Villereal, M.C. Rao, and E.B. Chang. 1994. A unique sodium-hydrogen exchange isoform (NHE-4) of the inner medulla of the rat kidney is induced by hyperosmolarity. *J. Biol. Chem.* 269:29704–29709.

32. Nader, N., G. Lamprecht, M. Classen, and U. Seidler. 1994. Different regulation by pH_i and osmolarity of the rabbit ileum brush-border and parietal cell basolateral anion exchanger. *J. Physiol. (Lond.)* 481:605–615.

33. Wang, Z., P.J. Schultheis, and G.E. Shull. 1996. Three N-terminal variants of the AE2 Cl^-/HCO_3^- exchanger are encoded by mRNAs transcribed from alternative promoters. *J. Biol. Chem.* 271:7835–7843.

34. Stuart-Tilley, A., C. Sardet, J. Pouyssegur, M.A. Schwartz, D. Brown, and S.L. Alper. 1994. Immunolocalization of anion exchanger AE2 and cation exchanger NHE-1 in distinct adjacent cells of gastric mucosa. *Am. J. Physiol.* 266:C559–C568.

35. Soybel, D.I., S.R. Gullans, F. Maxwell, and E. Delpire. 1995. Role of basolateral Na^+-K^+-Cl^- cotransport in HCl secretion by amphibian gastric mucosa. *Am. J. Physiol.* 269:C242–C249.

36. Lytle, C. 1997. Activation of the avian erythrocyte Na-K-Cl cotransport protein by cell shrinkage, cAMP, fluoride, and calyculin-A involves phosphorylation at common sites. *J. Biol. Chem.* 272:15069–15077.

37. Smith, P., P. O'Brien, D. Fromm, and W. Silen. 1977. Secretory state of gastric mucosa and resistance to injury by exogenous acid. *Am. J. Surg.* 133:81–85.

38. Kivilaakso, E., D. Fromm, and W. Silen. 1978. Effect of the acid secretory state on intramural pH of rabbit gastric mucosa. *Gastroenterology.* 75:641–648.

39. Starlinger, M., R. Jakesz, J.B. Matthews, C. Yoon, and R. Schiessel. 1981. The relative importance of HCO_3^- and blood flow in the protection of rat gastric mucosa during shock. *Gastroenterology.* 81:732–735.

40. Starlinger, M., and R. Schiessel. 1988. Bicarbonate (HCO_3) delivery to the gastroduodenal mucosa by the blood: its importance for mucosal integrity. *Gut.* 29:647–654.

41. Gannon, B., J. Browning, and P. O'Brien. 1982. The microvascular architecture of the glandular mucosa of rat stomach. *J. Anat.* 135:667–683.

42. Gannon, B., J. Browning, P. O'Brien, and P. Rogers. 1984. Mucosal microvascular architecture of the fundus and body of human stomach. *Gastroenterology.* 86:866–875.